

On the mechanical interaction between cellulose microfibrils and matrix substances in wood cell walls: effects of chemical pretreatment and subsequent repeated dry-and-wet treatment

Keisuke Toba · Hiroyuki Yamamoto ·
Masato Yoshida

Received: 16 January 2013 / Accepted: 26 April 2013 / Published online: 22 May 2013
© The Japan Wood Research Society 2013

Abstract We investigated the influences of chemical pretreatments and subsequent repeated dry-and-wet (RDW) treatments on the mechanical linkage between cellulose microfibrils (CMFs) and matrix substances (MT) in wood cell wall. Sugi (*Cryptomeria japonica* D. Don) quarter-sawn specimens were subjected to various types of chemical pretreatments, including ethanol and benzene extraction, delignification, alkali extraction, and hygrothermal treatment, to give substantial damages to principal constituents of wood cell wall, followed by 5 times of RDW treatment. After giving chemical pretreatment, the d -spacing of (200) lattice plane of cellulose I_{β} (d_{200}), the crystallinity of wood cell wall, and the crystal size of the cellulose were measured at the fiber saturated point, using X-ray diffraction techniques. Thereafter, these were measured again at the absolutely dried condition in the process of subsequent RDW treatments. The d_{200} in specimens, which were given to light pretreatments, largely expanded by drying at the early stages of RDW treatments, then it decreased and became constant after 5 times of RDW treatments. On the other hand, d_{200} in specimens, which were given to intensive pretreatments, remained constant at a relatively small level throughout the whole process of RDW treatments. After 5 times of RDW treatments, d_{200} became similar values between the above two groups. This suggests that RDW treatments have similar effects as intensive pretreatments, which induce substantial damages to the microscopic region in the wood cell wall such as interfacial separation between CMF, MT, and so

forth. These defects would weaken mechanical interaction between CMF and MT in the wood cell wall during drying.

Keywords Crystallinity · Crystal size · Lattice spacing · X-ray diffraction · Moisture adsorption

Introduction

Wood fiber is made of multi-layered cell walls which approximately consist of two-phase structure, i.e., rigid crystal of cellulose microfibrils (CMFs) and flexible matrix substances (MTs) of lignin, hemicellulose, and noncrystalline cellulose. The CMF, the size of which is a few nanometers in width [1], consists of dozens of β -1,4-glucan chains. Particularly in the secondary wall, which occupies most part of the cell wall, the CMF accumulates in a direction nearly parallel to the longitudinal axis of the wood fiber, while MT fills in the gaps between CMFs in each layer.

X-ray diffraction (XRD) technique is available for collecting information on the microstructure of crystalline materials [2, 3]. For example, some authors have adopted the XRD technique to detect the crystal lattice deformation induced by tensile or bending stress [4–6], moisture adsorption [7–15], cell wall maturation [16–18], and so forth. Among them, change in lattice spacing due to moisture adsorption is a quite interesting phenomenon. Toba et al. [15] pointed out the possibility that the CMF is laterally expanded by the shrinking MT during drying, and that binding force between CMF and MT is reduced after giving repeated drying and re-swelling treatments to the wood cell wall. Recently, some authors showed that repeated drying and re-swelling increase the crystallinity in wood cell wall [13, 19, 20]. These studies contain the

K. Toba · H. Yamamoto (✉) · M. Yoshida
Graduate School of Bioagricultural Sciences,
Nagoya University, Nagoya 464-8601, Japan
e-mail: hiro@agr.nagoya-u.ac.jp

information on the microscopic properties of the wood cell wall; thus, it is rather natural to consider that crystal lattice deformation is more or less correlated with increasing of the crystallinity, which is induced by repeated moisture change. However, no studies have focused on this problem yet, thus whole picture of fine structure in wood cell wall is still unaddressed.

It is well known that chemical treatments induce substantial change in the microscopic region of wood cell wall. For example, Jungnickel et al. [21] investigated the influences of delignification and subsequent alkali treatments on the spruce wood cell wall in terms of nanostructural organization, and they reported that visible size of CMF aggregation changed in the courses of chemical treatments. Fahlén and Salmén [22] observed that kraft pulp processing increased formation of nanoscale pores in wood cell wall, and at the same time, aggregation of cellulose fiber also became larger as observed by atomic force microscope. These studies imply that chemical treatment induces the changes in wood cell wall at the microscopic level, thus providing important information on the microscopic structure and behaviors of the interface between CMF and MT.

The purpose of the present study is to further understand the effects of repeated drying and re-swelling on the mechanical interaction between CMF and MT in wood cell wall, following our previous reports [18, 20]. Thus, we prepared specimens which were subjected to various types of pretreatments, that is, chemical extraction as well as hygrothermal treatment to give some damages to principal constituents of wood cell wall, followed by repeated dry-and-wet treatments. Based on the measurements of d -spacing of (200) lattice plane of cellulose I_{β} (d_{200}), the crystallinity, and the crystal size, we tried to clarify the microscopic behaviors of cell wall constituents, as well as interfacial structure between CMF and MT.

Materials and methods

Tested tree

The specimens studied were prepared from sap wood of 39-year-old sugi (*Cryptomeria japonica* D. Don), grown in Nagoya University Forest, Japan. The diameter at breast height was 24.0 cm. Oven-dried density was $0.31 \pm 0.02 \text{ g/cm}^3$ (mean \pm SD). Quarter-sawn specimen with dimensions of $2 \times 16 \times 15 \text{ mm}$ (thickness \times length \times width) was made from the tested tree. Figure 1 showed the process flow of subsequent treatments in the present study. For the purpose of inducing selective damages to the microscopic region in the cell wall, prior to repeated dry-and-wet (RDW) treatments, never-dried specimens were divided into eight groups without drying and were subjected to differing pretreatments: untreated (control), ethanol and benzene extraction, light and intensive delignification (2 or 6 h), light and intensive alkali extraction (soaked in 3 or 10 % of aqueous NaOH solution), and light and intensive hygrothermal treatments (120 or 140 °C). The details are as follows.

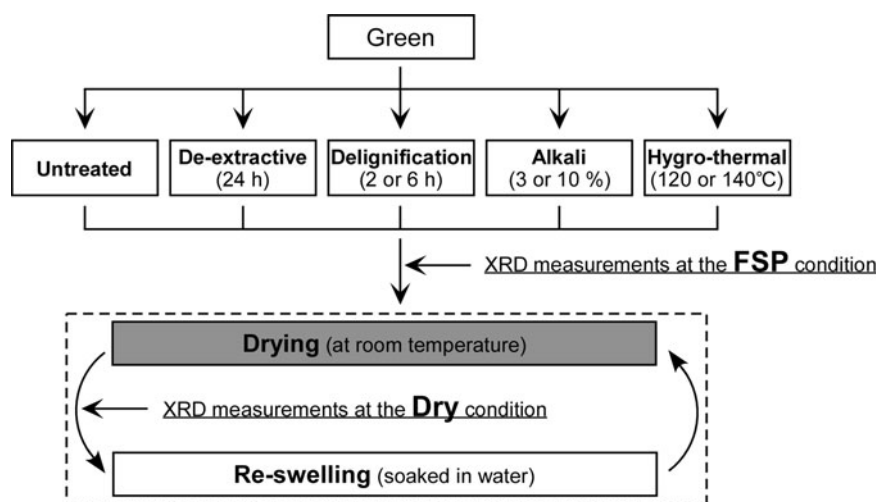
Ethanol and benzene extraction

Ethanol and benzene extracted specimens were prepared using Soxhlet extractor with refluxing a mixture of ethanol and benzene (1:2 v/v) for 24 h. After the extraction, mixed solvent was replaced by pure ethanol and then was replaced by distilled water in stages every second days (pure ethanol, 95, 90, 70, 50, 30, 10, and 0 %).

Delignification

Delignification specimens were prepared based on improved acid-chlorite method [23], which uses acetic acid buffer solution for the purpose of inhibiting outflow of

Fig. 1 Process flow for each type of pretreatment and subsequent RDW treatment. Rectangles with dashed lines indicate the processes that were repeated



polysaccharide during treatment. After 2 or 6 h of treatments, specimens were rinsed with running water for 1 week.

Alkali extraction

Alkali extracted specimens were prepared by soaking in 3 or 10 % concentration of aqueous NaOH solution for a month at room temperature. After the extraction, specimens were rinsed with running water for 1 week.

Hygrothermal treatment

Hygrothermal treated specimens were prepared using an autoclave at 120 or 140 °C for an hour. After the treatment, specimens still in the autoclave were cooled to room temperature.

Repeated dry-and-wet treatment

After giving each pretreatment, all specimens were conditioned in a sealed desiccator with distilled water, 100 % RH, for about 1 month until they reached equilibrium, which was considered as the fiber saturation point (FSP). The FSP is defined as the moisture content of wood specimen when cell wall is filled with bound water [24].

Subsequently, all specimens were given the RDW treatment. They were seasoned to the dry condition in a sealed desiccator with phosphorous (V) oxide for 1 week without heating, and then, they were soaked in distilled water at room temperature to make them re-swell again. This process of drying and re-swelling was repeated 5 times.

XRD measurements

XRD measurements were performed to assess the d -spacing of (200) lattice plane of cellulose I_{β} (d_{200}), the crystallinity, and the crystal size of (200) lattice plane of crystalline cellulose in wood cell wall at the FSP before and after pretreatments, and at each dry condition in the process of RDW treatments. Figure 2 describes a schematic of d_{200} of the crystalline cellulose in the wood cell wall. In the present study, detections of the peak positions of 110 and $1\bar{1}0$ diffractions were not performed. The authors consider that peak separation between 110 and $1\bar{1}0$ diffractions might cause some errors because these two peaks are too close to each other in wood cell wall. In addition, 200 diffraction peak is sharper than 110 and $1\bar{1}0$. Thus, we consider it is better to measure the d_{200} as an indicator of the transverse directional change of the cellulose crystals.

An X-ray diffractometer (XD-D1w, Shimadzu Co., Japan) was used to measure the crystalline properties under the following conditions. All XRD measurements were

made with the reflection technique. The incident X-ray radiation was the Cu $K\alpha$ characteristic X-ray passing through a nickel filter with a power of 30 kV and 30 mA. Both the air-scattering prevention slit and the divergence slit were 1°. The width of the detection slit was 0.1 mm. Scanning speed and integration time in the measurement of d_{200} were 0.125°/min and 0.4 s, respectively. On the other hand, those were 2.0°/min and 2.0 s in the measurement of the crystallinity and the crystal size, respectively. Scanning ranges of 2θ were 21.5°–23.2° in the d_{200} and 5.0°–40.0° in the crystallinity and the crystal size. Quarter-sawn specimens were vertically fixed on the sample holder of XRD device to irradiate radial section. Moisture-conditioned air was circulated through the specimen cabinet mounted on the turntable to prevent the specimen from changing moisture content during measurements.

The d_{200} was calculated using the Bragg equation, as follows:

$$d_{200} = \frac{\lambda}{2 \sin \theta_{200}} \quad (1)$$

where λ is the incident X-ray wavelength (0.1542 nm), and θ_{200} is the Bragg angle (°) on the basis of the peak position of 200 diffraction obtained from the diffraction diagram. The peak position of silicon powder was used to remove the error in 2θ angle measurements. To confirm the significant figure in the measurement of diffraction angle, we performed repeated measurements using silicon powder ($2\theta \cong 28.445^\circ$). As a result, significant value in 2θ angle measurement was limited in the range of 0.0001°.

Since wood contains a large amount of crystalline cellulose, we can regard the wood as a crystalline material. In the present study, the degree of crystallinity in wood cell wall was calculated using Segal method [25], as follows:

$$C_S = \frac{I_{200} - I_{Am}}{I_{200}} \times 100 (\%) \quad (2)$$

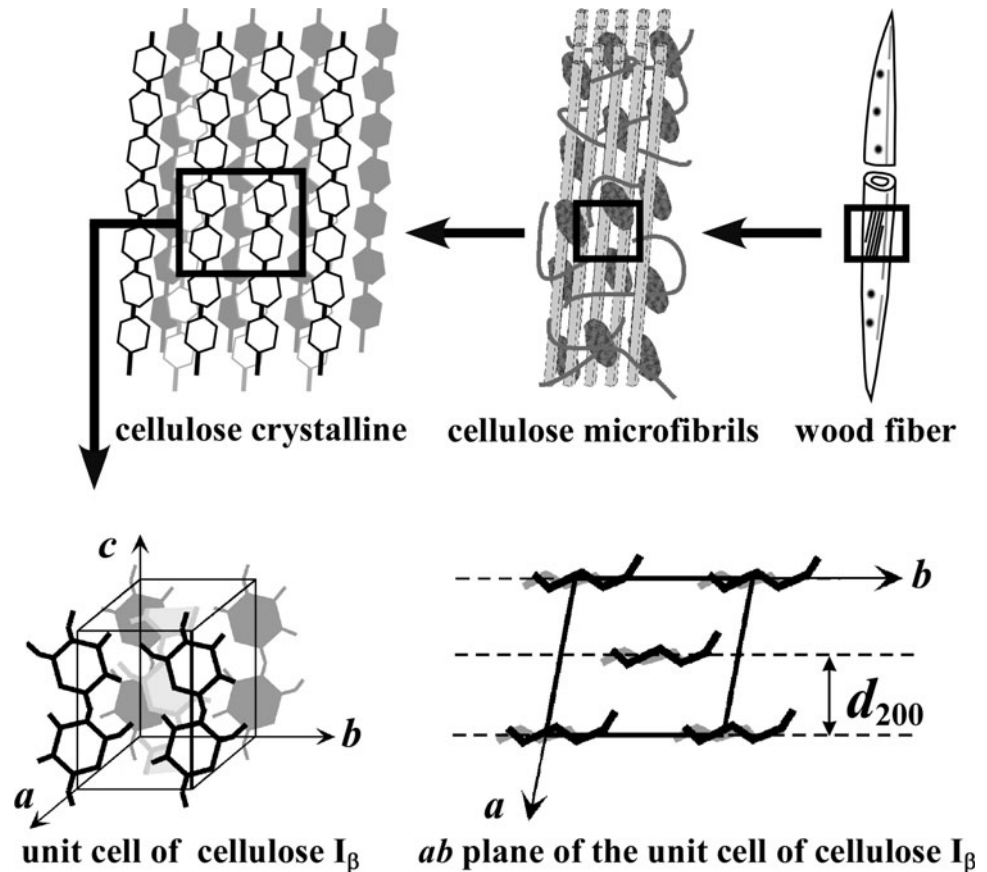
where C_S was the crystallinity (%) of wood cell wall, I_{200} is the reflection intensity of 200 diffraction, and I_{Am} is the intensity at the minimum near 18.5° of 2θ angle. Segal method is simple to be applied and do not require peak separation between 110 and $1\bar{1}0$ diffraction. We consider that Segal method is sufficient to estimate the crystallinity in the case of investigating not the absolute content of crystal but the qualitative changes of cellulose in wood cell wall.

The size of cellulose crystal was calculated on the basis of the Scherrer equation [3], as follows:

$$D_{200} = \frac{K\lambda}{B \cos \theta_{200}} \quad (3)$$

where D_{200} is the crystal size (nm) for (200) plane diffraction, K the Scherrer constant (0.9), λ the incident X-ray

Fig. 2 Cellulose microfibrils which compose of wood cell wall and d_{200} in crystalline structure



wavelength (0.1542 nm), B the half bandwidth in radians, and θ_{200} is the Bragg angle ($^{\circ}$) for (200) plane.

Results and discussion

d -Spacing of (200) lattice plane of cellulose I_{β} (d_{200})

Figure 3 shows variations of d_{200} induced by each pretreatment and subsequent RDW treatments. Based on the changes of d_{200} due to treatment, crystal strain (ε_{200}) was calculated from the following equation:

$$\varepsilon_{200} = \frac{d'_{200} - d_{200}^{\text{Green}}}{d_{200}^{\text{Green}}} \times 100 (\%) \quad (4)$$

where d_{200}^{Green} is d_{200} (nm) of green specimen at the FSP and d'_{200} is the one after giving each pretreatment or subsequent RDW treatments. Table 1 shows the results in ε_{200} .

First, slight increases in d_{200} were observed after each pretreatment (Fig. 3b–h). The ε_{200} was 0.09–0.19 % in each pretreatment, as shown in Table 1. In our previous paper, we reported that boiling treatment changed the d_{200} in the green wood cell wall, which was caused by relaxing the growth stress remaining in microscopic region of wood cell wall; as a result, 0.15–0.18 % of ε_{200} was observed

[18]. This coincides with ε_{200} observed after pretreatments in the present study. These suggest that each pretreatment in the present study would act in a similar manner to boiling treatment, leading to the increase in d_{200} .

Figure 3a shows the results of untreated specimen. The d_{200} largely expanded due to initial drying. However, it gradually decreased and then became constant in the process of RDW treatments. This trend of variation in d_{200} was reported also in our previous study [15]. In the present study, it was found that light pretreated specimens (Fig. 3b, c, e, g) showed similar trend of variation in d_{200} as untreated specimens, while intensive pretreated specimens (Fig. 3d, f, h) showed constant value at a relatively small level throughout the whole process of RDW treatments. It should be noted that d_{200} in all specimens became uniform 0.3988 ± 0.0002 nm after giving 5 times of RDW treatments.

We consider that shrinking MT in untreated or light pretreated specimens has an ability to give a lateral tensile stress to the CMF in the drying process (Fig. 3b, c, e, g). As a result, d_{200} largely expands with drying. However, this tensile stress was gradually reduced in the process of RDW treatments. On the other hand, tensile stress in intensive pretreated specimens has been already weakened from the beginning of RDW treatment (Fig. 3d, f, h). This reduction of tensile stress to the CMF at drying suggests that repeated

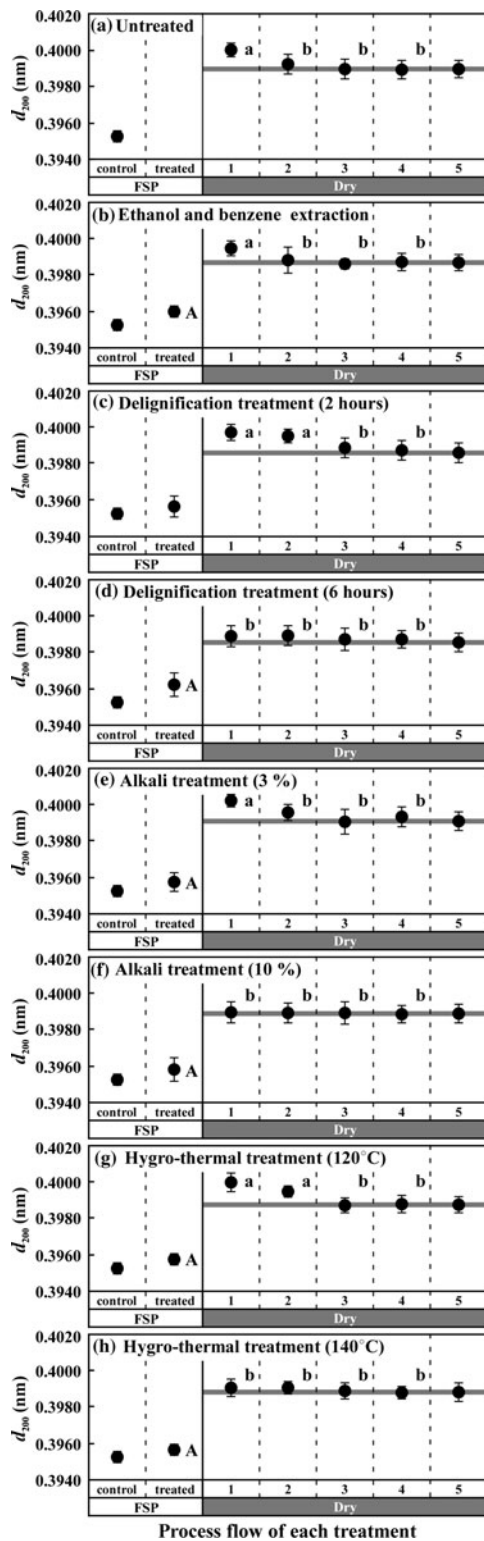


Fig. 3 Variations of d_{200} induced by each pretreatment and subsequent repeated dry-and-wet (RDW) treatments. In this figure, “A” indicates that there was significant difference $<5\%$ level between before and after pretreatment. “a” indicates that there were significant differences $<5\%$ level compared to the fifth RDW treatment. “b” shows no significance compared to the fifth RDW treatment. A gray solid line indicates the level of d_{200} after the fifth RDW treatment in each case

Table 1 Crystal strains ϵ_{200} (%) induced by each pretreatment and subsequent RDW treatments

Treatments	Number of specimen	ϵ_{200} (%)					
		After pretreatment					
		FSP	Dry 1	Dry 2	Dry 3	Dry 4	
Untreated	10	-	1.22	1.02	0.95	0.94	0.94
De-extractive	10	0.18	1.10	0.90	0.84	0.87	0.87
Delignification (2 h)	10	0.09	1.11	1.03	0.97	0.87	0.85
Delignification (6 h)	10	0.19	0.92	0.93	0.88	0.89	0.90
Alkali treatment (3 %)	10	0.12	1.26	1.10	0.97	1.04	0.97
Alkali treatment (10 %)	10	0.14	0.94	0.93	0.94	0.91	0.93
Hygrothermal treatment (120 °C)	10	0.12	1.20	1.06	0.87	0.90	0.89
Hygrothermal treatment (140 °C)	10	0.09	0.96	0.97	0.92	0.90	0.90

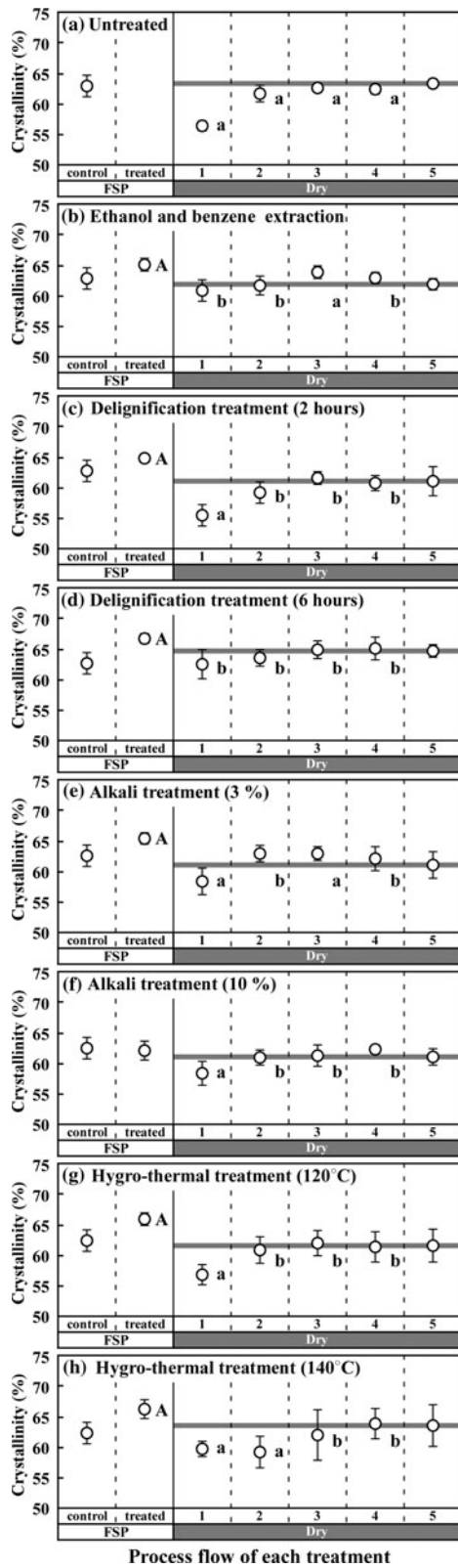


Fig. 4 Variation of crystallinity of wood cell wall induced by each pretreatment and subsequent repeated dry-and-wet (RDW) treatments. “A”, “a” and “b” show same meaning as in Fig. 3. A gray solid line indicates the level of the crystallinity after the fifth RDW treatment in each case

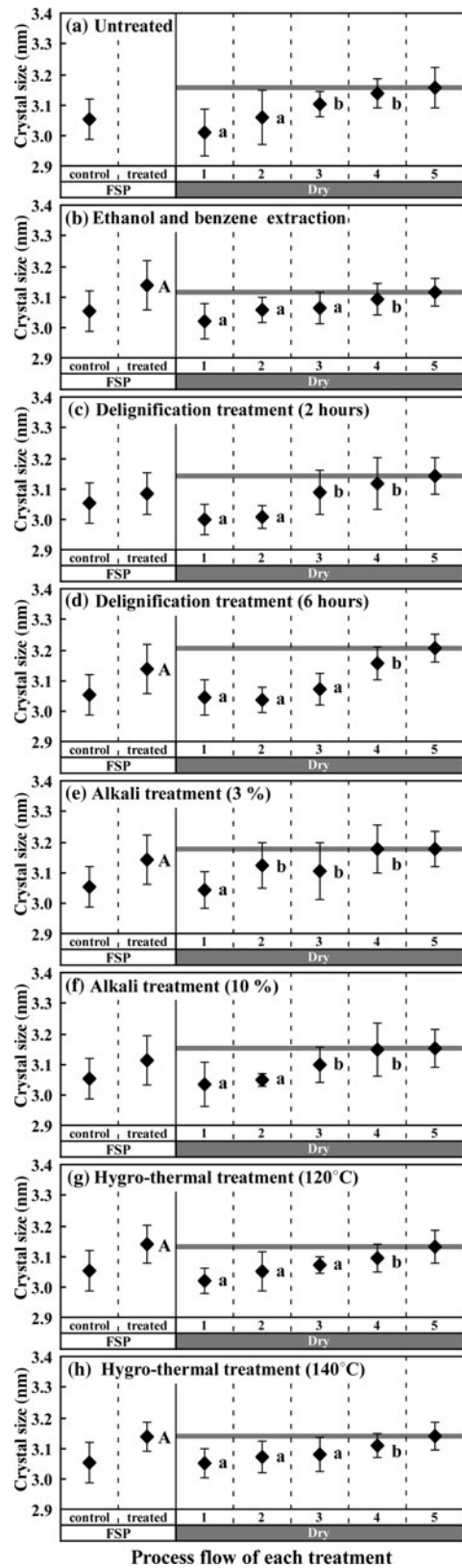


Fig. 5 Variation of crystal size induced by each pretreatment and subsequent repeated dry-and-wet (RDW) treatments. “A”, “a” and “b” show same meaning as in Fig. 3. A gray solid line in each case indicates the level of the crystal size after the fifth RDW treatment

moisture changing produced the same effect as that of giving intensive pretreatment.

On comparing the average value of ε_{200} before and after giving 5 times of RDW treatments, it was reduced up to 26 %. If the changes in d_{200} would be a simple elastic deformation, it is natural to consider that RDW treatments decreased the ability of the MT to give lateral tensile stress to the CMF at the drying process. Concretely to say, each pretreatment or subsequent RDW treatments gave substantial damage to the cell wall in microscopic region, such as outflow or degradation of the constituents in the MT, interfacial separation between CMF and MT, and so forth. These damages weakened mechanical interaction between CMF and MT. It is considered that the above differences in values of d_{200} in the earlier stages of RDW treatments depend on the extent of the defect caused by pretreatments.

Crystallinity and crystal size

Figures 4 and 5 show variations of the crystallinity and the crystal size induced by each pretreatment and subsequent RDW treatments, respectively. The crystallinity and the crystal size at the FSP increased after each pretreatment (Figs. 4b–h, 5b–h). Outflow or degradation of the MT is one of the possible factors to cause increases in the crystallinity and the crystal size. Increases of the crystallinity and the crystal size were also shown in Figs. 4b and 5b (24 h of ethanol and benzene extraction treatment). However, sugi contains at most 3 % of extractives, which are soluble in mixture of ethanol and benzene. The amounts are much lower than those of cellulose, hemicellulose, and lignin. This indicates that increases in the crystallinity and the crystal size, as shown in Figs. 4b and 5b, were not merely attributed to removal of ethanol and benzene soluble extractives, but also to changing in the relative ratio of crystalline component in whole wood cell wall.

Thereafter, both the crystallinity and the crystal size decreased due to subsequent drying in all specimens. After that, RDW treatments were performed on the specimens. On the whole, the crystallinity showed two types of variations in the process of RDW treatments. Some showed smaller values of the crystallinity in the early stage of RDW treatments, and then, it became higher in the later stage (Fig. 4a, b, c, e, g). Others kept higher values from the beginning throughout 5 times of RDW treatments (Fig. 4d, f, h). Latter type was observed in specimens which were given intensive pretreatments. However, the crystallinity in both types became constant at the end of RDW treatments. It is considered that differences in the crystallinity between the above two types reflect the extent of damage of MT caused by each pretreatment. On the other hand, the crystal size kept increasing even after the crystallinity became constant in all specimens (Fig. 5).

The results of crystalline properties suggest that RDW treatments have similar effects as pretreatments, which induce substantial damages to the microscopic region in wood cell wall. In addition, repeated changing of moisture content in wood cell wall creates the condition to promote the crystallization of cellulose in wood cell wall, as reported in our previous paper [20]. We consider that non-crystalline cellulose, which contains a large amount of free hydroxyl groups, forms additional hydrogen bonding in the process of RDW treatments. Extent of hydrogen bonding increased after repeated moisture changing. Intensive pretreatments, which produced certain damages in microscopic region of the cell wall (e.g., interfacial separation between the CMF and MT), create the condition to accelerate hydrogen bonding formation in noncrystalline cellulose. This is the reason why the crystallinity of wood cell wall showed higher values from the beginning of RDW treatment in intensive pretreated specimens (Fig. 4d, f, h).

Our idea remains a matter of speculation. However, it would be natural to consider that some sorts of substantial damages arise in microscopic region in wood cell wall because absolute dried weight of specimen remained constant throughout 5 times of RDW treatments. For total understanding of the mechanism of phenomena observed in this study, step-up investigation will be required, e.g., comparing the physical properties of RDW-treated wood with thermal-dried wood, aged wood, and so forth [26, 27].

Acknowledgments The authors greatly appreciate cooperation of Mr. Yasuji Imaizumi, Mr. Naoki Takabe, and Mr. Norio Yamaguchi from the Nagoya University Experimental Forest for their assistance in logging the sample trees.

References

1. Fengel D, Wegener G (1984) Wood. Chemistry, ultrastructure, reactions. Walter de Gruyter, New York
2. Hengstenberg J, Mark H (1928) Röntgenunter suchungen über fen bau der C-Ketten in kohlenwass-erstoffen. Z krist 67:583
3. Alexander LE (1969) X-ray diffraction in polymer science. Wiley-Interscience, New York
4. Moriizumi S, Okano T (1978) Viscoelasticity and structure of wood. 4. Behavior of crystal lattice strain depended on moisture content and time. Mokuzai Gakkaishi 24:1–6
5. Nakai T, Yamamoto H, Nakao T, Hamatake M (2006) Mechanical behavior of the crystal lattice of natural cellulose in wood under repeated uniaxial tension stress in the fiber direction. Wood Sci Technol 40:683–695
6. Montero C, Clair B, Almérás T, van der Lee A, Gril J (2012) Relationship between wood elastic strain under bending and cellulose crystal strain. Compos Sci Technol 72:175–181
7. Sobue N, Shibata Y, Mizusawa T (1992) X-ray measurement of lattice strain of cellulose crystals during the shrinkage of wood in the longitudinal direction. Mokuzai Gakkaishi 38:336–341
8. Abe K, Yamamoto H (2005) Mechanical interaction between cellulose microfibril and matrix substance in wood cell wall determined by X-ray diffraction. J Wood Sci 51:334–338

9. Abe K, Yamamoto H (2006) Change in mechanical interaction between cellulose microfibril and matrix substance in wood cell wall induced by hygrothermal treatment. *J Wood Sci* 52:107–110
10. Sugino H, Sugimoto H, Miki T, Kanayama K (2007) Fine structure changes of wood during moisture adsorption and desorption process analyzed by X-ray diffraction measurement. *Mokuzai Gakkaishi* 53:82–89
11. Peura M, Kölln K, Grotkopp I, Saranpää P, Müller M, Serimaa R (2007) The effect of axial strain on crystalline cellulose in Norway spruce. *Wood Sci Technol* 41:565–583
12. Zabler S, Paris O, Burgert I, Fratzl P (2010) Moisture changes in the plant cell wall force cellulose crystallites to deform. *J Struct Biol* 171:133–141
13. Hill SJ, Kirby NM, Mudie ST, Hawley AM, Ingham B, Franich RA, Newman RH (2010) Effect of drying and rewetting of wood on cellulose molecular packing. *Holzforchung* 64:421–427
14. Leppänen K, Bjurhager I, Peura M, Kallonen A, Suuronen JP, Penttilä P, Love J, Fagerstedt K, Serimaa R (2012) X-ray scattering and microtomography study on the structural change of never-dried silver birch, European aspen and hybrid aspen during drying. *Holzforchung* 65:865–873
15. Toba K, Yamamoto H, Yoshida M (2012) Mechanical interaction between cellulose microfibrils and matrix substances in wood cell walls induced by repeated wet-and-dry treatment. *Cellulose* 19:1405–1412
16. Clair B, Alméras T, Yamamoto H, Okuyama T, Sugiyama J (2006) Mechanical behavior of cellulose microfibrils in tension wood, in relation with maturation stress generation. *Biophys J* 91:1128–1135
17. Clair B, Alméras T, Pilate G, Jullien D, Sugiyama J, Riekel C (2011) Maturation stresses generation in poplar tension wood studied by synchrotron radiation microdiffraction. *Plant Physiol* 155:562–570
18. Toba K, Yamamoto H, Yoshida M (2013) Micromechanical detection of growth stress in wood cell wall by wide-angle X-ray diffraction (WAX). *Holzforchung* 67:315–323
19. Olek W, Bonarski J (2012) Influence of cyclic sorption on wood ultrastructure. *Bioresources* 7:1729–1739
20. Toba K, Yamamoto H, Yoshida M (2013) Crystallization of cellulose microfibrils in wood cell wall by repeated dry-and-wet treatment, using X-ray diffraction technique. *Cellulose* 20:633–643
21. Jungnickel K, Paris O, Fratzl P, Burgert I (2008) The implication of chemical extraction treatments on the cell wall nanostructure of softwood. *Cellulose* 15:407–418
22. Fahlén J, Salmén L (2005) Pore and matrix distribution in the fiber wall revealed by atomic force microscopy and image analysis. *Biomacromolecules* 6:433–438
23. Maekawa E, Koshijima T (1983) Evaluation of the acid-chlorite method for the determination of wood Holocellulose. *Mokuzai Gakkaishi* 29:702–707
24. Kollmann FFP, Côté WA (1984) Principles of wood science and technology. Solid wood, vol 1. Springer, Berlin
25. Segal L, Creely JJ, Martin AE, Conrad CM (1959) An empirical method for estimating the degree of crystallinity of native cellulose using the X-ray diffractometer. *Textile Res J* 29:786–794
26. Matsuo M, Yokoyama M, Umemura K, Gril J, Yano K, Kawai S (2010) Color changes in wood during heating: kinetic analysis by applying a time-temperature superposition method. *Appl Phys A* 99:47–52
27. Noguchi T, Obataya E, Ando K (2012) Effects of aging on the vibrational properties of wood. *J Cult Herit* 13(Supplement):s21–s25